

Universal precursor of superconductivity in the cuprates

Yu, G.; Xia, D.-D.; Pelc, D.; He, R.-H.; Kaneko, N.-H.; Sasagawa, T.; Li, Y.; Zhao, X.; Barišić, N.; Shekhter, A.; ...

Source / Izvornik: **Physical Review B, 2019, 99**

Journal article, Published version

Rad u časopisu, Objavljena verzija rada (izdavačev PDF)

<https://doi.org/10.1103/PhysRevB.99.214502>

Permanent link / Trajna poveznica: <https://urn.nsk.hr/urn:nbn:hr:217:468820>

Rights / Prava: [In copyright](#) / [Zaštićeno autorskim pravom.](#)

Download date / Datum preuzimanja: **2024-07-14**



Repository / Repozitorij:

[Repository of the Faculty of Science - University of Zagreb](#)



Universal precursor of superconductivity in the cuprates

G. Yu,^{1,*} D.-D. Xia,^{1,2,†} D. Pelc,^{1,3} R.-H. He,⁴ N.-H. Kaneko,⁵ T. Sasagawa,⁶ Y. Li,⁷ X. Zhao,^{1,2} N. Barišić,^{3,8,‡}
A. Shekhter,^{9,§} and M. Greven^{1,||}

¹*School of Physics and Astronomy, University of Minnesota, Minneapolis, Minnesota 55455, USA*

²*State Key Lab of Inorganic Synthesis and Preparative Chemistry, College of Chemistry, Jilin University, Changchun 130012, China*

³*Department of Physics, Faculty of Science, University of Zagreb, Bijenička cesta 32, HR-10000, Zagreb, Croatia*

⁴*Westlake Institute for Advanced Study, Hangzhou 310024, Zhejiang, China*

⁵*National Institute of Advanced Industrial Science and Technology (AIST), 1-1-1 Umezono, Tsukuba, Ibaraki 305-8563, Japan*

⁶*MSL, Tokyo Institute of Technology, Kanagawa 226-8503, Japan*

⁷*International Center for Quantum Materials, School of Physics, Peking University, Beijing 100871, China*

⁸*Institute of Solid State Physics, TU Wien, 1040 Vienna, Austria*

⁹*Pulsed Field Facility, National High Magnetic Field Laboratory, Los Alamos National Laboratory, Los Alamos, New Mexico 87545, USA*



(Received 12 May 2018; revised manuscript received 14 May 2019; published 10 June 2019)

Using torque magnetometry, we reveal remarkably simple universal behavior of the superconducting (SC) precursor in the cuprates by tracking the nonlinear diamagnetism above T_c in four distinct compounds: single-CuO₂-layer HgBa₂CuO_{4+δ}, La_{2-x}Sr_xCuO₄ and Bi₂(Sr,La)₂CuO_{6+δ}, and double-layer Bi₂Sr₂Ca_{0.95}Y_{0.05}Cu₂O_{8+δ}. We find that SC diamagnetism vanishes in an exponential manner, characterized by a universal temperature scale that is approximately independent of compound and T_c . We discuss the possibility that this unusual behavior signifies the proliferation of SC clusters as a result of intrinsic inhomogeneity inherent to the cuprates.

DOI: [10.1103/PhysRevB.99.214502](https://doi.org/10.1103/PhysRevB.99.214502)

I. INTRODUCTION

High- T_c superconductivity in the cuprates emerges from a metallic state that exhibits unusual pseudogap phenomena [1]. One of the pivotal open questions is how superconductivity emerges from this complex state. For the extensively studied systems La_{2-x}Sr_xCuO₄ (LSCO), Bi₂(Sr,La)₂CuO_{6+δ} (Bi2201), and YBa₂Cu₃O_{6+δ} (YBCO), some experiments (Nernst effect [2,3], torque magnetization [4–6], photoemission [7], infrared spectroscopy [8]) seem to indicate signatures of superconductivity in an anomalously wide temperature range above T_c in the underdoped part of the phase diagram. Yet other experiments (microwave [9,10], terahertz conductivity [11–14], and specific heat [15]) reveal signatures of incipient superconductivity only in a relatively narrow temperature range above T_c . Furthermore, extensive recent work has focused on the interplay between superconductivity and other ordering tendencies, including the possibility of a simultaneous appearance of superconducting and charge-density-wave (CDW) fluctuations relatively far above T_c [1,16]. One of the experimental problems is that it is difficult to disentangle the SC response from other ordering tendencies,

e.g., the Nernst signal can be strongly affected by CDW fluctuations [17]. Therefore, it has been challenging to reliably establish the normal-state behavior and hence to unambiguously extract the SC signal. Recent nonlinear conductivity [18] and paraconductivity [19] measurements provide further evidence that traces of superconductivity indeed vanish rapidly above T_c , in an exponential fashion. Such temperature dependence is incompatible with prevailing theoretical ideas but consistent with an inhomogeneous SC gap distribution, i.e., with local superconductivity above T_c and with SC percolation [18,19].

In this paper, we use torque magnetometry to study the precursor SC diamagnetism above T_c . Torque magnetometry is a thermodynamic probe with extremely high sensitivity to SC diamagnetism, a fundamental characteristic of superconductivity [20]. Upon considering the nonlinear magnetic field dependence, we find that the SC diamagnetism can be unambiguously disentangled from the normal-state paramagnetism. We investigate nonlinear diamagnetism in HgBa₂CuO_{4+δ} (Hg1201), LSCO, Bi2201, and Bi₂Sr₂Ca_{0.95}Y_{0.05}Cu₂O_{8+δ} (Bi2212), with a focus on the doping dependence of Hg1201 and on a direct comparison of all four compounds near optimal doping. Hg1201 is a model single-layer compound [21–26] that features a simple tetragonal crystal structure, minimal extrinsic disorder effects, and an optimal transition temperature T_c^{\max} of nearly 100 K. We demonstrate that the precursor SC diamagnetism in all four cuprates is nearly indistinguishable, despite the dramatically lower T_c^{\max} values of LSCO and Bi2201 (just below 40 K [21]) and the double-layer nature of Bi2212. The nonlinear diamagnetism follows exponential-like rather than power-law temperature dependence on $T - T_c$, in a universal (nearly compound

*Present address: Informatics Institute, University of Minnesota, Minneapolis, Minnesota 55455, USA; yug@umn.edu

†Present address: Shenyang Pharmaceutical University, Shenyang 110016, China

‡barisic@ifp.tuwien.ac.at

§Present address: National High Magnetic Field Laboratory, Tallahassee, Florida 32310, USA.

||greven@umn.edu

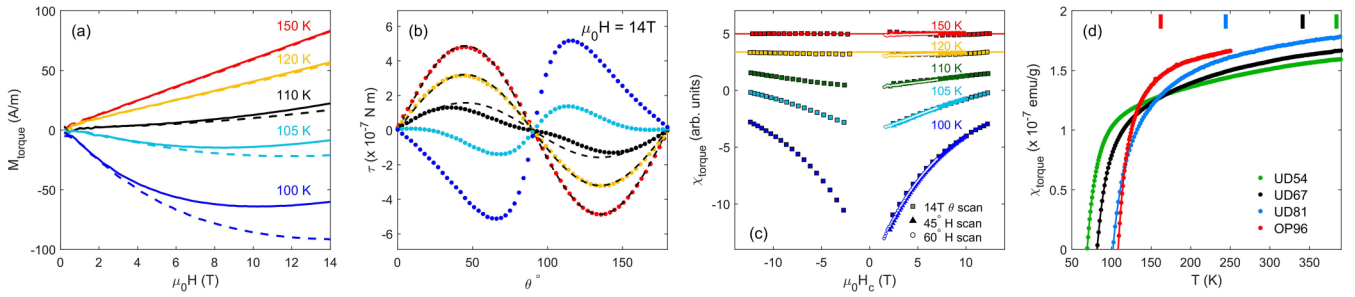


FIG. 1. Data for Hg1201. (a) Field dependence of the effective magnetic moment $M_{\text{torque}} \equiv \chi_{\text{torque}} H$ at $\theta = 45^\circ$ (solid lines) and 60° (dashed lines) for a nearly optimally doped sample OP96 ($T_c \approx 96$ K). M_{torque} equals the effective magnetic moment $M_{\text{eff}} \equiv \tau / (\mu_0 V H \sin(\theta))$ defined in [4,5] divided by $\cos(\theta)$. $M_{\text{eff}} = M_c - M_a H_c / H_a$ approximates the c -axis magnetization M_c when the in-plane magnetization M_a is negligible. Unlike M_{eff} , M_{torque} is independent of angle θ for linear magnetism. Therefore, the discrepancy of M_{torque} between two different angles at temperatures below 120 K is a clear indication of the appearance of nonlinear magnetism. (b) Angular dependence of the torque for OP96. The temperature is indicated by the same colors as in (a). The deviation from the $\sin(2\theta)$ dependence occurs below the same temperature as the onset of the nonlinear component of M_{torque} in (a). Dashed black lines are fits to $\sin(2\theta)$ for 150, 120, and 110 K. (c) χ_{torque} as a function of H_c for OP96, calculated from the field dependence in (a) (triangles: $\theta = 45^\circ$; circles: $\theta = 60^\circ$) and from the angular dependence in (b) (squares: $\mu_0 H = 14$ T). The two methods agree remarkably well, which indicates that the result is hardly affected by H_a . The contribution from the in-plane response thus is negligible, and χ_c dominates the nonlinear diamagnetic signal in this temperature range. Horizontal lines at 120 K and 150 K indicate the field-independent paramagnetic contributions. (d) χ_{torque} over a wide temperature range above T_c for OP96 and three underdoped samples UD54, UD67, and UD81 ($T_c \approx 54, 67, 81$ K). χ_{torque} is obtained with an external magnetic field $\mu_0 H = 14$ T at $\theta = 45^\circ$. At high temperature, in the normal state, M_{torque} is independent of θ , and χ_{torque} (now equal to $\chi_c - \chi_a$) is independent of θ and H up to at least 14 T with very good accuracy. The vertical bars indicate the pseudogap temperature T^* estimated from neutron scattering [35,36] and planar dc resistivity measurements [42]. Nontrivial temperature dependences of χ_{torque} (and $d\chi_{\text{torque}}/dT$) are observed up to 400 K. Similar behavior as in (a)–(d) is observed for the other cuprates [28].

independent) manner, in excellent agreement with the recent complementary linear and nonlinear conductivity results [18,19].

II. EXPERIMENTAL DETAILS

Hg1201 crystals were grown as previously described [27] and annealed in an oxygen rich or poor atmosphere to achieve the desired doping levels [22]. Optimally-doped Bi2201 ($T_c = 35$ K) and underdoped Bi2212 ($T_c = 90$ K) crystals were grown by the traveling-solvent floating-zone technique [21]. The quoted onset T_c values for all samples were determined from zero-field-cooled susceptibility measurements in 5 Oe magnetic field oriented along the crystallographic c axis. For Bi2201 and Bi2212, p is estimated from the empirical relation $T_c/T_c^{\text{max}} = 1 - 82.6 \times (p - 0.16)^2$. For LSCO, we use $p = x$.

The torque measurements were carried out with high-sensitivity torque lever chips, using Quantum Design, Inc., PPMS instruments. In torque magnetometry, the magnetization \mathbf{M} is deduced from the mechanical torque $\tau = V\mu_0(\mathbf{M} \times \mathbf{H})$ experienced by a crystal in a magnetic field \mathbf{H} . Here, μ_0 is the permeability of free space and V is the sample volume. The torque is measured as a function of temperature, magnetic field, and orientation of the sample with respect to the field direction. For a tetragonal system such as Hg1201 (and for nearly tetragonal systems such as LSCO, Bi2201, and Bi2212 [28]), the sample orientation is parameterized by the angle θ between \mathbf{H} and the crystallographic c -axis. The field dependence of the magnetization can be obtained either directly, through field scans at a fixed angle, or indirectly, by observing the angular dependence

of the torque in a fixed field. In the angular scans, the linear-in-field magnetization (paramagnetic or diamagnetic) reveals itself as the second harmonic in the angular dependence, $\tau \propto H^2 \sin(2\theta)$, whereas the non-linear-in-field magnetization introduces higher harmonics. For clarity, we define the torque susceptibility $\chi_{\text{torque}}(H, \theta, T) = \tau / (V\mu_0 H_a H_c) = M_c / H_c - M_a / H_a (\propto \tau / (H^2 \sin(2\theta)))$, where $H_a = H \sin(\theta)$ and $H_c = H \cos(\theta)$ are the components of \mathbf{H} along the crystallographic a and c directions, and M_c (M_a) is the magnetization component along the c -axis (in-plane) direction. In the linear response regime, $\chi_{\text{torque}}(T)$ equals the susceptibility anisotropy $\chi_c(T) - \chi_a(T)$ and is independent of field strength and orientation of the crystal. For non-linear-in-field response, such as SC diamagnetism, χ_{torque} varies with H and θ .

III. RESULTS

In the normal state, at sufficiently high temperatures, we find for all samples perfect linear-in-field paramagnetic response in both the field and angular scans up to 14 T, the highest field of our study. Whereas pseudogap phenomena (e.g., $q = 0$ magnetic order [35,36], CDW order [1,37–39], and nematic order [40,41]) may affect the magnitude of the paramagnetic susceptibility, the linear-in-field paramagnetic response holds with great precision below the respective characteristic temperatures. This is demonstrated for Hg1201 in Figs. 1(a)–1(c), both via direct observation of the magnetization as well as via consideration of χ_{torque} , and indicative of the absence of any SC diamagnetism. In contrast to the normal-state response, the SC diamagnetism manifests itself via the nonlinear magnetic field dependence, even in relatively low fields [Fig. 1(c)]. For example, for a Hg1201 crystal with

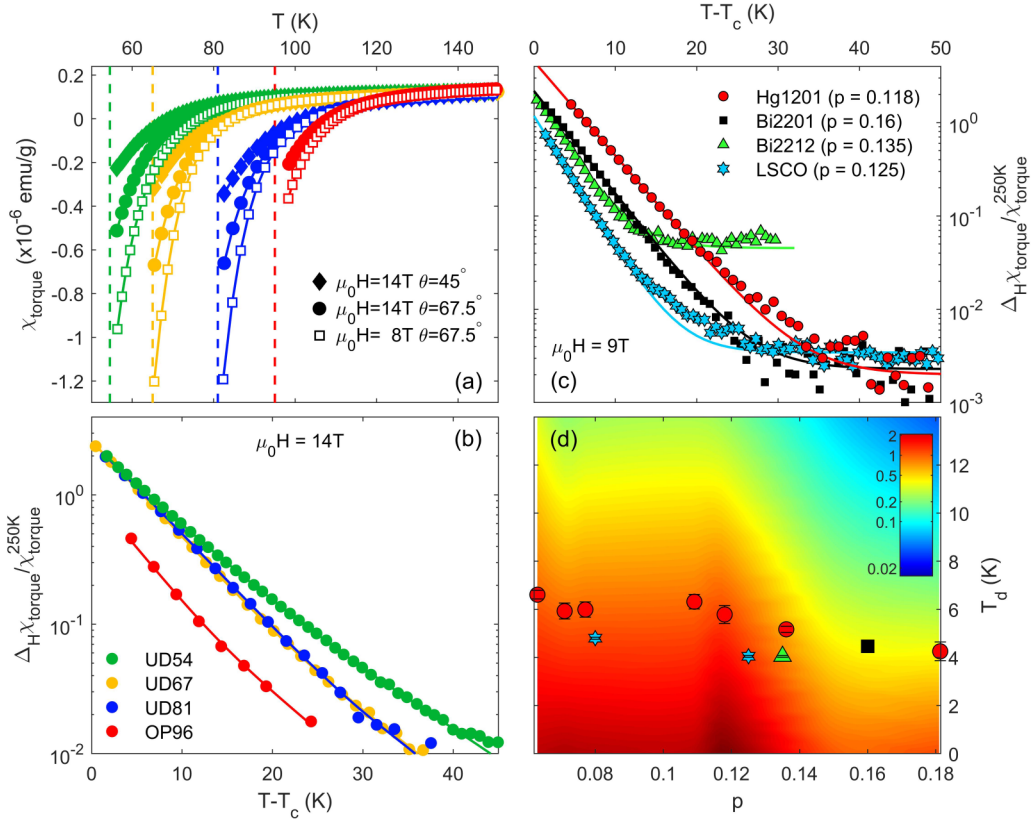


FIG. 2. Universal behavior of the torque susceptibility. (a) $\chi_{\text{torque}}(H, \theta, T)$ obtained under three different conditions for Hg1201 samples UD54, UD67, UD81, and OP96: (i) $\mu_0 H = 14$ T, $\theta = 45^\circ$; (ii) $\mu_0 H = 14$ T, $\theta = 67.5^\circ$; (iii) $\mu_0 H = 8$ T, $\theta = 45^\circ$. Deviations upon approaching T_c are due to SC diamagnetism. Vertical dashed lines indicate zero-field T_c . $\Delta_H \chi_{\text{torque}}$ can be evaluated as either the difference between (i) and (ii) or (i) and (iii). (b) $\Delta_H \chi_{\text{torque}}(T) \equiv \chi_{\text{torque}}(14 \text{ T}, 45^\circ, T) - \chi_{\text{torque}}(14 \text{ T}, 67.5^\circ, T)$ for Hg1201 [from (a)], normalized at 250 K, versus $T - T_c$ (T_c values were obtained in the limit of zero magnetic field). Lines in (a) and (b) are guides to the eye. (c) Comparison of $\Delta_H \chi_{\text{torque}} \equiv \chi_{\text{torque}}(9 \text{ T}, 45^\circ, T) - \chi_{\text{torque}}(9 \text{ T}, 67.5^\circ, T)$ for slightly underdoped Hg1201 ($p = 0.118$, $T_c = 89$ K), LSCO ($p = x = 0.125$, $T_c = 27$ K), Bi2212 ($p = 0.135$, $T_c = 90$ K), and optimally doped Bi2201 ($p = 0.16$, $T_c = 35$ K). Solid lines are fits to an exponential behavior plus a small constant corresponding to the sensitivity limit [28]. (d) Characteristic temperature of SC diamagnetism, T_d , vs hole concentration for Hg1201 (circles), Bi2201 (square), Bi2212 (triangle), and LSCO (stars) extracted for $\mu_0 H_c$ in the range 3.1–3.4 T from $\chi_{\text{torque}} \propto \exp(T/T_d)$ near T_c . T_d is nearly independent of compound and decreases slightly with increasing p . Errors represent fit uncertainties [28]. The color contour shows the magnitude of the nonlinear magnetic response $\log_{10}(\Delta_H \chi_{\text{torque}} / \chi_{\text{torque}}^{250\text{K}})$ for Hg1201 as a function of $T - T_c$ and p . Normalization of $\Delta_H \chi_{\text{torque}}$ by its high-temperature value allows the comparison of samples with different hole concentrations [28]. T_d weakly increases with increasing H_c , but this does not affect the observation of universal behavior. Whereas T_d is best defined from χ_{torque} , the difference $\Delta_H \chi_{\text{torque}}$ used in Figs. 2, S2, and S3 (Ref. [28]) better demonstrates the exponential decay and gives a better estimate of the measurable extent of SC traces.

$T_c \approx 96$ K, the nonlinear magnetization in the field scans and the higher harmonics in the angular scans are clearly discernible below the same temperature of about 120 K [Figs. 1(a) and 1(b)].

The temperature dependence of χ_{torque} for Hg1201, Bi2201, and LSCO (Figs. 1(d) and 2(a) and Figs. S3 and S4 in Ref. [28]) reveals two distinct behaviors above T_c . The near- T_c regime is clearly dominated by SC diamagnetism and features an approximately exponential decay, accompanied by a strong nonlinear field dependence of the magnetization [Figs. 1(a)–1(c)]. At higher temperatures, χ_{torque} exhibits qualitatively different temperature dependence and no magnetic field dependence (within our sensitivity limit) and thus is clearly identified as normal-state paramagnetism. Previous torque studies of LSCO and Bi2201 [4–6] deduced SC diamagnetism by subtracting an assumed high-temperature T -linear background, $\chi(T) = (a + bT)$. This assumption

yields apparent diamagnetism in an anomalously wide temperature range above T_c , very different from early torque studies [43–45]. Our data do not support this assumption [see Fig. 1(d)]. Furthermore, we find that the nonlinear signal is present in the entire field range of our measurements, indicated by the continuously varying χ_{torque} as a function of field [Fig. 1(c)]. This implies that dominant linear-in-field SC diamagnetism can only appear below the lowest field of our measurements. Therefore, the discrepancy with the previous torque studies [4–6] is not due to the existence of a dominant linear-in-field SC diamagnetic response.

Without resorting to any assumptions regarding the paramagnetic response, we identify SC diamagnetism from the difference ($\Delta_H \chi_{\text{torque}}$) of χ_{torque} at two different fields (or, equivalently, at two different angles), which completely removes the paramagnetic (i.e., linear response) component and leaves only nonlinear magnetism. This enables us to

trace the SC diamagnetism at temperatures well above T_c , even when the SC signal is two orders of magnitude smaller than the high-temperature paramagnetic magnetization. As shown in Figs. 2(b) and 2(c), we find that $\Delta_H \chi_{\text{torque}}$ exhibits a rapid exponential decrease with increasing temperature, $\Delta_H \chi_{\text{torque}} \propto \exp(-T/T_d)$, where T_d is a measure of the temperature range over which SC traces are significant. Figures 2(b) and 2(d) demonstrate for Hg1201 that T_d exhibits weak doping dependence from the very underdoped ($p \approx 0.07$) to the overdoped ($p \approx 0.18$) part of the phase diagram.

Our measurements of optimally-doped Bi2201 and moderately underdoped LSCO reveal that the diamagnetic response of all three single-layer compounds is nearly indistinguishable [Figs. 2(c), 2(d) S2, S3], despite the stark difference (a factor of about 2.5) in T_c^{max} and the prominent charge/spin stripe correlations in $x = 0.125$ LSCO [1]. The universal nature of the observed behavior is further demonstrated for double-layer Bi2212 [$T_c \approx 90$ K; Figs. 2(c) and 2(d)].

IV. DISCUSSION

These results are significant for a number of reasons. First, they constitute an unequivocal thermodynamic determination of SC emergence in the cuprates, as we observe SC emergence directly via diamagnetism, a fundamental and prominent characteristic of superconductivity [20], and because our experimental approach does not resort to any “background” estimation. Second, they indicate that the emergence of superconductivity (χ_{torque}) exhibits highly unusual yet robust exponential temperature dependence with a characteristic temperature T_d that is clearly independent of T_c . Contrary to the interpretation of recent torque results for $\text{Bi}_2\text{Sr}_2\text{CaCu}_2\text{O}_{8+\delta}$ [6] and $\text{YBa}_2\text{Cu}_3\text{O}_{6+x}$ [46], this behavior cannot be described by Ginzburg-Landau theory, in which T_c is the characteristic fluctuation temperature scale and which predicts an approximately power-law temperature dependence [20]. Third, we demonstrate that the scale T_d is universal (compound independent). In particular, near optimal doping, the nonlinear diamagnetic response of all four investigated cuprate families is characterized by exponential decay with $T_d = 4\text{--}5$ K. Fourth, this is the case even for $p = 0.125$ LSCO, where stripe correlations are particularly prominent, and for Hg1201 in the $p = 0.07\text{--}0.11$ range, where CDW correlations are prominent in this compound [37–39]. This implies that these correlations are not directly relevant to SC emergence and that they must have inadvertently affected a number of prior results [2–7,47]. Moreover, we note that in quantum-critical-point scenarios, SC pairing is mediated by the fluctuations of a distinct order parameter [1], yet the observed behavior for overdoped Hg1201 near the putative quantum critical point at $p \approx 0.19$ is the same as at low doping. The extensive data for the model cuprate Hg1201 allow us to establish that the diamagnetism at temperatures above T_c closely tracks the $T_c(p)$ dome and thus is unrelated to the various ordering tendencies that appear at or below the pseudogap temperature $T^*(p)$ [35–39,41], which monotonically decreases with increasing doping. Last, but not least, the observation of an exponential decay of the SC response with a universal characteristic temperature scale is fully consistent with recent

nonlinear conductivity [18] and paraconductivity [19] results. This implies the existence of an underlying characteristic temperature (or energy scale) proportional to T_d and independent of T_c .

How can we understand the unusual SC emergence? The cuprates are lamellar, perovskite-derived materials that are inhomogeneous at the nanoscale [48–54], and even simple-tetragonal Hg1201 exhibits considerable variation in local electric field gradients and structure [50,51]. These complex oxides exhibit microstructural (“tweed” or “transformation precursor”) patterns commonly found in many displacive, diffusionless structural transformations (e.g., perovskites and martensitic systems) as a result of stress accommodation. The associated mechanical strain inhomogeneity should result in prominent electronic features, since charge and spin degrees of freedom naturally couple to strain [48,49]. Evidence for inhomogeneity is observed on multiple energy scales, ranging from about 0.1 eV in scanning tunneling microscopy (STM) to 10^{-7} eV in nuclear magnetic resonance measurements. STM demonstrates that both the pseudogap [52–54] and the lower-energy SC gap [53,54] exhibit considerable spatial inhomogeneity. Consequently, some of the spatially inhomogeneous SC gaps “survive” in the form of SC clusters at temperatures well above T_c . As the temperature decreases, these clusters proliferate, grow in size, and eventually percolate near T_c . The emergence of superconductivity may therefore be thought of as a percolation process, with a temperature scale controlled by the distribution of the SC gap rather than by T_c . A recent phenomenological model based on inhomogeneous, temperature-, and doping-dependent (de)localization of one hole per planar CuO_2 unit can explain the main features of the normal-state phase diagram [55]. It is conceivable that the universal scale T_d uncovered in our torque measurements corresponds to the width of the superconducting gap distribution and emerges via a complex renormalization of these high-energy localization (pseudo)gaps. On the other hand, point disorder varies from compound to compound [21] and thus cannot be directly relevant to our observations.

Quantitative evaluation of the nonlinear torque signal is difficult within the percolation scenario, and beyond the scope of the present work, as it would involve the temperature and magnetic-field dependence of the SC gap distribution, the size distribution of the SC clusters, and the Josephson coupling among the clusters. Nevertheless, we note that the recent conductivity measurements show universal exponential behavior as well and that in this case the comparison with a simple percolation model is greatly simplified because small isolated SC clusters do not contribute to the conductance and large clusters dominate the response [18,19]. The linear paraconductivity exhibits exponential decay with a characteristic temperature that is nearly identical to T_d from our torque measurements [19], and both linear and nonlinear (third-harmonic) conductivity can be quantitatively described by a simple percolation model [18,19]. This demonstrates that the exponential temperature dependence can indeed be described by a percolation process. As noted, such a description fits well into an overarching picture of cuprate physics, where the key element is intrinsic localization-gap inhomogeneity [55]. The SC gap distribution discussed here can then be understood as

a manifestation of the same underlying inhomogeneity on a lower, emergent energy scale.

ACKNOWLEDGMENTS

We thank P.A. Crowell for the use of the 9 T Quantum Design, Inc., Physical Properties Measurement System (PPMS). The 14 T data were obtained with a PPMS in the Geballe Laboratory for Advanced Materials at Stanford University. The work on Hg1201 was funded by the Depart-

ment of Energy through the University of Minnesota Center for Quantum Materials, under DE-SC-0016371. The work on Bi2201 and LSCO was supported by NSF Grant No. 1006617 and by the NSF through the University of Minnesota MRSEC under Grant No. DMR-1420013. The work at the TU Wien was supported by FWF project P27980-N36 and the European Research Council (ERC Consolidator Grant No. 725521). The work at the Jilin University was supported by National Natural Science Foundation of China (Grant No. 21371068).

- [1] B. Keimer, S. A. Kivelson, M. R. Norman, S. Uchida, and J. Zaanen, *Nature (London)* **518**, 179 (2015).
- [2] Z. A. Xu, N. P. Ong, Y. Wang, T. Kakeshita, and S. Uchida, *Nature (London)* **406**, 486 (2000).
- [3] Y. Wang, L. Li, and N. P. Ong, *Phys. Rev. B* **73**, 024510 (2006).
- [4] Y. Wang, L. Li, M. J. Naughton, G. D. Gu, S. Uchida, and N. P. Ong, *Phys. Rev. Lett.* **95**, 247002 (2005).
- [5] L. Li, Y. Wang, S. Komiyama, S. Ono, Y. Ando, G. D. Gu, and N. P. Ong, *Phys. Rev. B* **81**, 054510 (2010).
- [6] H. Xiao, T. Hu, W. Zhang, Y. M. Dai, H. Q. Luo, H. H. Wen, C. C. Almasan, and X. G. Qiu, *Phys. Rev. B* **90**, 214511 (2014).
- [7] T. Kondo, Y. Hamaya, A. D. Palczewski, T. Takeuchi, J. S. Wen, Z. J. Xu, G. Gu, J. Schmalian, and A. Kaminski, *Nat. Phys.* **7**, 21 (2011).
- [8] A. Dubroka, M. Rössle, K. W. Kim, V. K. Malik, D. Munzar, D. N. Basov, A. A. Schafgans, S. J. Moon, C. T. Lin, D. Haug, V. Hinkov, B. Keimer, T. Wolf, J. G. Storey, J. L. Tallon, and C. Bernhard, *Phys. Rev. Lett.* **106**, 047006 (2011).
- [9] M. S. Grbić, N. Barišić, A. Dulčić, I. Kupčić, Y. Li, X. Zhao, G. Yu, M. Dressel, M. Greven, and M. Požek, *Phys. Rev. B* **80**, 094511 (2009).
- [10] M. S. Grbić, M. Požek, D. Paar, V. Hinkov, M. Raichle, D. Haug, B. Keimer, N. Barišić, and A. Dulčić, *Phys. Rev. B* **83**, 144508 (2011).
- [11] L. S. Bilbro, R. V. Aguilar, G. Logvenov, O. Pelleg, I. Božović, and N. P. Armitage, *Nat. Phys.* **7**, 298 (2011).
- [12] D. Nakamura, Y. Imai, A. Maeda, and I. Tsukada, *J. Phys. Soc. Jpn.* **81**, 044709 (2012).
- [13] R. Corson, L. Mallozzi, J. Orenstein, J. N. Eckstein, and I. Božović, *Nature (London)* **398**, 221 (1999).
- [14] J. Orenstein, J. Corson, S. Oh, and J. N. Eckstein, *Ann. Phys.* **15**, 596 (2006).
- [15] H.-H. Wen, G. Mu, H. Luo, H. Yang, L. Shan, C. Ren, P. Cheng, J. Yan, and L. Fang, *Phys. Rev. Lett.* **103**, 067002 (2009).
- [16] E. Fradkin, S. A. Kivelson, and J. M. Tranquada, *Rev. Mod. Phys.* **87**, 457 (2015).
- [17] O. Cyr-Choinière, R. Daou, F. Laliberté, D. LeBoeuf, N. Doiron-Leyraud, J. Chang, J.-Q. Yan, J.-G. Cheng, J.-S. Zhou, J. B. Goodenough, S. Pyon, T. Takayama, H. Takagi, Y. Tanaka, and L. Taillefer, *Nature (London)* **458**, 743 (2009).
- [18] D. Pelc, M. Vučković, M. S. Grbić, M. Požek, G. Yu, T. Sasagawa, M. Greven, and N. Barišić, *Nat. Commun.* **9**, 4327 (2018).
- [19] P. Popčević, D. Pelc, Y. Tang, K. Velebit, Z. Anderson, V. Nagarajan, G. Yu, M. Požek, N. Barišić, and M. Greven, *npj Quantum Materials* **3**, 42 (2018).
- [20] S. A. Kivelson and E. H. Fradkin, *Physics* **3**, 15 (2010).
- [21] H. Eisaki, N. Kaneko, D. L. Feng, A. Damascelli, P. K. Mang, K. M. Shen, Z.-X. Shen, and M. Greven, *Phys. Rev. B* **69**, 064512 (2004).
- [22] N. Barišić, Y. Li, X. Zhao, Y.-C. Cho, G. Chabot-Couture, G. Yu, and M. Greven, *Phys. Rev. B* **78**, 054518 (2008).
- [23] M. K. Chan, M. J. Veit, C. J. Dorow, Y. Ge, Y. Li, W. Tabis, Y. Tang, X. Zhao, N. Barišić, and M. Greven, *Phys. Rev. Lett.* **113**, 177005 (2014).
- [24] N. Barišić, S. Badoux, M. K. Chan, C. Dorow, W. Tabis, B. Vignolle, G. Yu, J. Béard, X. Zhao, C. Proust, and M. Greven, *Nat. Phys.* **9**, 761 (2013).
- [25] M. K. Chan, N. Harrison, R. D. McDonald, B. J. Ramshaw, K. A. Modic, N. Barišić, and M. Greven, *Nat. Commun.* **7**, 12244 (2016).
- [26] Y. Li, N. Egetenmeyer, J. L. Gavilano, N. Barišić, and M. Greven, *Phys. Rev. B* **83**, 054507 (2011).
- [27] X. Zhao, G. Yu, Y.-C. Cho, G. Chabot-Couture, N. Barišić, P. Bourges, N. Kaneko, Y. Li, L. Lu, E. Motoyama, O. Vajk, and M. Greven, *Adv. Mater.* **18**, 3243 (2006).
- [28] See Supplemental Material at <http://link.aps.org/supplemental/10.1103/PhysRevB.99.214502> which includes supplementary text, supplementary Figs. S1-S6, and Refs. [29–34].
- [29] C. M. Varma, *Phys. Rev. B* **73**, 155113 (2006).
- [30] J. M. Tranquada, B. J. Sternlieb, J. D. Axe, Y. Nakamura, and S. Uchida, *Nature (London)* **375**, 561 (1995).
- [31] F. Rullier-Albenque, H. H. Alloul, and G. Rikken, *Phys. Rev. B* **84**, 014522 (2011).
- [32] J. Bobroff, H. Alloul, S. Ouazi, P. Mendels, A. Mahajan, N. Blanchard, G. Collin, V. Guillen, and J.-F. Marucco, *Phys. Rev. Lett.* **89**, 157002 (2002).
- [33] J. B. Goodenough and A. Manthiram, *J. Solid State Chem.* **88**, 115 (1990).
- [34] J. B. Goodenough, *Supercond. Sci. Technol.* **3**, 26 (1990).
- [35] Y. Li, V. Balédent, N. Barišić, Y. Cho, B. Fauqué, Y. Sidis, G. Yu, X. Zhao, P. Bourges, and M. Greven, *Nature (London)* **455**, 372 (2008).
- [36] Y. Li, V. Balédent, N. Barišić, Y. C. Cho, Y. Sidis, G. Yu, X. Zhao, P. Bourges, and M. Greven, *Phys. Rev. B* **84**, 224508 (2011).
- [37] W. Tabis, Y. Li, M. Le Tacon, L. Braicovich, A. Kreyssig, M. Minola, G. Dellea, E. Weschke, M. J. Veit, M. Ramazanoglu, A. I. Goldman, T. Schmitt, G. Ghiringhelli, N. Barišić, M. K. Chan, C. J. Dorow, G. Yu, X. Zhao, B. Keimer, and M. Greven, *Nat. Commun.* **5**, 5875 (2014).
- [38] W. Tabis, B. Yu, I. Bialo, M. Bluschke, T. Kolodziej, A. Kozłowski, E. Blackburn, K. Sen, E. M. Forgan, M. v. Zimmermann, Y. Tang, E. Weschke, B. Vignolle, M. Hepting,

- H. Gretarsson, R. Sutarto, F. He, M. Le Tacon, N. Barišić, G. Yu, and M. Greven, *Phys. Rev. B* **96**, 134510 (2017).
- [39] J. P. Hinton, E. Thewalt, Z. Alpichshev, F. Mahmood, J. D. Koralek, M. K. Chan, M. J. Veit, C. J. Dorow, N. Barišić, A. F. Kemper, D. A. Bonn, W. N. Hardy, R. Liang, N. Gedik, M. Greven, A. Lanzara, and J. Orenstein, *Sci. Rep.* **6**, 23610 (2016).
- [40] Y. Sato, S. Kasahara, H. Murayama, Y. Kasahara, E.-G. Moon, T. Nishizaki, T. Loew, J. Porras, B. Keimer, T. Shibauchi, and Y. Matsuda, *Nat. Phys.* **13**, 1074 (2017).
- [41] H. Murayama, Y. Sato, R. Kurihara, S. Kasahara, Y. Mizukami, Y. Kasahara, H. Uchiyama, A. Yamamoto, E.-G. Moon, J. Cai, J. Freyermuth, M. Greven, T. Shibauchi, and Y. Matsuda, [arXiv:1805.00276](https://arxiv.org/abs/1805.00276) [Nat. Commun. (to be published)].
- [42] N. Barišić, M. K. Chan, Y. Li, G. Yu, X. Zhao, M. Dressel, A. Smontara, and M. Greven, *Proc. Natl. Acad. Sci. USA* **110**, 12235 (2013).
- [43] C. Bergemann, A. W. Tyler, A. P. Mackenzie, J. R. Cooper, S. R. Julian, and D. E. Farrell, *Phys. Rev. B* **57**, 14387 (1998).
- [44] M. J. Naughton, *Phys. Rev. B* **61**, 1605 (2000).
- [45] J. Hofer, T. Schneider, J. M. Singer, M. Willemin, H. Keller, T. Sasagawa, K. Kishio, K. Conder, and J. Karpinski, *Phys. Rev. B* **62**, 631 (2000).
- [46] I. Kokanović, D. J. Hills, M. L. Sutherland, R. Liang, and J. R. Cooper, *Phys. Rev. B* **88**, 060505(R) (2013).
- [47] P. M. C. Rourke, I. Mouzopoulou, X. Xu, C. Panagopoulos, Y. Wang, B. Vignolle, C. Proust, E. V. Kurganova, U. Zeitler, Y. Tanabe, T. Adachi, Y. Koike, and N. E. Hussey, *Nat. Phys.* **7**, 455 (2011).
- [48] J. A. Krumhansl, Fine scale mesostructures in superconducting and other materials, in *Proceedings of the Conference of the Lattice Effects in High-Tc Superconductors, 13 to 15 January 1992* (World Scientific, Singapore, 1992).
- [49] J. C. Phillips, A. Saxena, and A. R. Bishop, *Rep. Prog. Phys.* **66**, 2111 (2003).
- [50] S. Agrestini, N. L. Saini, G. Bianconi, and A. Bianconi, *J. Phys. A: Math. Gen.* **36**, 9133 (2003).
- [51] D. Rybicki, J. Haase, M. Greven, G. Yu, Y. Li, Y. Cho, and X. Zhao, *J. Supercond. Novel Magn.* **22**, 179 (2009).
- [52] K. K. Gomes, A. N. Pasupathy, A. Pushp, S. Ono, Y. Ando, and A. Yazdani, *Nature (London)* **447**, 569 (2007).
- [53] M. C. Boyer, W. D. Wise, K. Chatterjee, M. Yi, T. Kondo, T. Takeuchi, H. Ikuta, and E. W. Hudson, *Nat. Phys.* **3**, 802 (2007).
- [54] J. W. Alldredge, K. Fujita, H. Eisaki, S. Uchida, and K. McElroy, *Phys. Rev. B* **87**, 104520 (2013).
- [55] D. Pelc, P. Popčević, M. Požek, M. Greven, and N. Barišić, *Sci. Adv.* **5**, eaau4538 (2019).